African Journal for Industrial and Applied Mathematics
Afr. J. Ind. Appl. Math., Vol. 1 , No. 1 , pp. 1-19

DOI: 10.4208/ajiam.2025-0001
June 2025

Mathematical Study of Fractional Magnetohydrodynamic Blood Flow Nanofluid in Activation of Thermal Radiation with Wright Function

R. Essono[1,*], T. C. Kofané[2] and C. B. Tabi[3]

[1] *National Advanced School of Maritime and Ocean Sciences and Technology, University of Ebolowa, PO Box 292 Kribi, Cameroon*
[2] *Laboratoire de Mécanique, Département de Physique, Faculté des Sciences, Université de Yaoundé I, BP 812 Yaoundé, Cameroun*
[3] *Botswana International University of Science and Technology, Private Bag 16 Palapye, Botswana*

Received 17 January 2025; Accepted (in revised version) 30 March 2025

Abstract. A study of magnetohydrodynamics model of blood flow is made with single walls carbon nanotubes, copper (Cu), tin (TiO_2), and alumina (Al_2O_3) and Cu as base nanoparticles through a circular cylinder. The fluid inside the tube is acted by an oscillating pressure gradient and an external constant magnetic field. The whole study is based on a mathematical model that includes Caputo fractional-order derivatives. Solutions for the blood velocitie, blood temperature distribution, and blood concentration distribution are obtained through the Laplace transform and expressed by the Wright function. Effects of the fractional-order parameter, magnetic field, the magnetic parameter M, the Grashof numbers Gr and Gm, the dimensionless time t, and the Prandtl parameter Pr are addressed using numerical simulations. Results show that the applied magnetic field reduces the velocities of the fluid and particles. However, under long time intervals, particles seem to be accelerated, but their velocity is suitably controlled by the fractional-order parameter.

AMS subject classifications: 35422, 44A10, 33E99, 76-10, 34K38

Keywords: Nanoparticles, Caputo fractional order derivatives, Wright function.

1 Introduction

Biomagnetic fluid dynamic (BFD) is a new area of research in mechanical fluid [30]. The transportation of drugs, cell separation devices, control of bleeding during surg-

*Corresponding author. *Emails:* essonorene@gmail.com (R. Essono), tabic@biust.ac.bw (C. B. Tabi), tckofane@gmail.com (T. C. Kofané)

eries and treatment of cancer tumors are efficiently done by biomagnetic fluids [12,21]. The inclusion of nanomaterials in the base fluid is an attracting technique that have been invented by scientists to improve the thermal efficiency [30]. In 1995, nanofluids introduced by Choi and Eastman [6] have received a considerable attention in current times. Nanofluids are essentially a combination of nano-sized objects contained in a fluid, name base fluid, that increases the thermal characteristics due to the collaboration of these nanomaterials [13].

Blood is a biomagnetic fluid, due to the strong presence of the erythrocytes playing the role of magnetic particles and the plasma as liquid carrier. The magnetization of blood can be augmented by adding artificially created nanoparticles to the flow as usually done in drug targeting delivery. One of the work addressed to the aspect of drug targeting was done in [11], where they studied the mechanism of magnetic targeting of carrier particles in the microvasculature for therapeutic uses. Biofluids should be considered as a medium that exhibits high electrical conductivity [10,15], especially when additional magnetic particles are injected in blood to carry drugs. This fact may justify the use of the principles of magnetohydrodynamics (MHD) [8, 10], which rely on the generation of Lorentz forces, in elaborating suitable mathematical models. Sharma *et al.* [25] studied for example the effect of external uniform magnetic field on flow parameters of both blood and magnetic particles based on a mathematical model using the MHD approach. Magnetic drug targeting (MDT) technique was used by Bose and Banerjee [3], where fluid hydrodynamic and MHD principles were coupled to track the magnetic particles under the effect of a magnetic field. Kefayati [17] studied the effect of a magnetic field on non-Newtonian blood flow between two-square concentric duct annuli, and further extended the study to non-Newtonian blood flow in a cavity driven by the motion of two facing lids [18]. In both cases, the results showed that the increment of Reynolds number augments the magnetic field effect on the flow of blood.

MDT is an interesting topic of research to be continued for discovering a better and improved method of drug delivery by employing a new factor based on the fractional calculus. Fractional calculus is one of the generalizations of classical calculus and it has been successfully applied in the various fields of science and engineering [5, 27–29, 31]. The studies [22, 28, 29] examined the effects of the fractional-order and magnetic fields on the flow of blood in a cylindrical domain by replacing the time derivative of order one with the Caputo fractional derivatives.

Motivated by the above investigations the present paper aims to study the combined heat and mass effects on an unsteady model of MHD blood flow. The objective of the present work is to study a mathematical model of blood flow in presence of magnetic particles and blood temperature, using Caputo fractional derivatives [4, 23]. External magnetic effects are considered and the blood in the vessel is assumed to be acted by a periodic pressure gradient. The mathematical model, which includes Caputo fractional derivatives, is generalized from the model containing integer derivatives, and solutions for the blood velocity, particle velocity and blood temperature are obtained by only making use of Laplace transform. Since Laplace transform expres-

sions of velocity, temperature and concentration are not classical functions, the inverse Laplace transform is difficult to find traditionally.

This paper is organized as follows. A brief description of the problem formulation is given in Section 2. The exact solutions of the partial differential equation governing the model are derived in Sections 3 and 4. The results are displayed in profiles and discussion are provided in Section 5. The conclusions of the paper are given in Section 6.

2 Description of the problem and formulation

We consider an unstable viscous transient one dimensional MHD blood and incompressible nanofluid on a cylindrical vessel, together with magnetic particles Fig. 1. We consider that magnetic particle to be uniformly distributed in the blood, the resulting ensemble flows in the axial direction x of the vessel. It is assumed that the Reynolds number is very small, hence the induced magnetic field is very neglected compare to the apply magnetic field. The particles, the tube and the blood inside are supposed to be at rest at $t < 0$. The particles, the tube and the blood inside are supposed to be at rest at $t = 0$. Particles are subjected to an electromotive force resulting from the interaction of current with the magnetic field. Its expression can be found in [14, 20, 25, 28] in the form

$$\overrightarrow{f}_{em} = -\sigma B_0^2 U(r,t)\overrightarrow{i} \tag{2.1}$$

with $\overrightarrow{i}$ being the unit vector in the $x-$direction and $U(r,t)$ the axial velocity of the blood, B_0 is the uniform magnetic field σ the electrical conductivity. We assume that the internal dissipation is absent and the usual Boussinesq approximation is taken into consideration. As a result the governing equations of momentum, energy, and concentration are derived as follows [1, 2, 19, 24, 28]:

$$\begin{aligned}\rho_{nf}\frac{\partial u^\star}{\partial t} &= -\frac{\partial p^\star}{\partial z} + \nu_{nf}\frac{\partial^2}{\partial r^{\star 2}}u^\star - \sigma_{nf}B_0^2 u \\ &\quad + g(\beta_T)_{nf}(T^\star - T_\infty^\star) + g(\beta_C)_{nf}(C^\star - C_\infty^\star),\end{aligned} \tag{2.2}$$

$$(\rho C_T)_{nf}\frac{\partial T^\star}{\partial t^\star} = k_{nf}\frac{\partial^2}{\partial r^{\star 2}}T^\star - \frac{\partial q}{\partial r^*}, \tag{2.3}$$

$$\frac{\partial C^\star}{\partial t^\star} = D_B\frac{\partial^2 C^\star}{\partial r^{\star 2}} + \frac{D_T}{T_\infty^\star}\frac{\partial^2 T^\star}{\partial r^{\star 2}}, \tag{2.4}$$

where $u^\star$ stands for the axial velocity, $T^\star$ and $C^\star$are respectively the temperature and the concentration of the solute, B_0 is the applied magnetic field, g, σ_{nf} and ρ_{nf} are respectively the acceleration due to gravity, electrical conductivity, and density of blood, $C_{Tnf}, k_{nf}$and ν_{nf} represent respectively the specific heat at constant pressure, thermal conductivity and kinematic viscosity, D_B and D_T are respectively the molecular diffusivity and the thermophoretic diffusion coefficient. In this system of equation, p is the

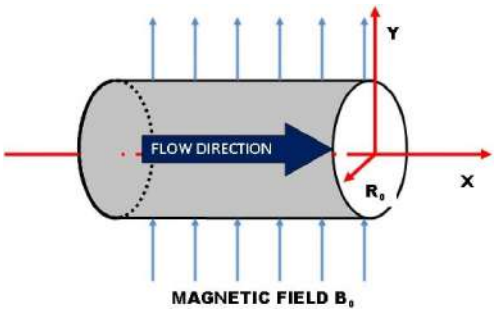

Figure 1: Schematic representation of the model geometry.

blood pressure, the oscillating gradient $\partial p/\partial x$ is given by

$$-\frac{\partial p}{\partial x} = b_0^* + b_1^* \cos(\omega t^*), \quad t^* > 0, \tag{2.5}$$

where b_0 and b_1 are the amplitude of the systolic and diastolic pressure gradient, respectively [19, 25, 30], with ω being the frequency. The radiative flux q_r is written assuming that blood is an optically thin fluid with a relatively low density and heat absorption coefficient. The radiative flux q_r can then be simplified as proposed by [7,26] in the form

$$\frac{\partial q}{\partial r^*} = -\frac{4\sigma^*}{3\beta_R}\frac{\partial T^*}{\partial r^*}, \tag{2.6}$$

where σ^* is the Stefan-Boltzmann fluid constant and β_R is the coefficient of mean absorption.

In this study, the base fluid is blood with single walls carbon nanotubes (SWCNTs), copper, tin, and alumina and copper as base nanoparticles [16, 22], Table 1. The coefficient of thermal of thermal expansion the density of nanofluid are taken to be

$$\begin{aligned}
\nu_{nf} &= \frac{\nu_f}{(1-\phi)^{2.5}},\\
\frac{k_{nf}}{k_f} &= \frac{\big(k_p + (m-1)k_f\big) - (m-1)\phi(k_f - k_p)}{\big(k_p + (m-1)k_f\big) + \phi(k_f - k_p)},\\
\rho_{nf} &= (1-\phi)\rho_f + \phi\rho_p,\\
\frac{\sigma_{nf}}{\sigma_f} &= 1 + \frac{3(\sigma_p/\sigma_f - 1)\phi}{(\sigma_p/\sigma_f + 2) - \phi(\sigma_p/\sigma_f - 1)},\\
(\rho\beta)_{nf} &= (1-\phi)(\rho\beta)_f + \phi(\phi\beta)_p,\\
\rho_{nf} &= (1-\phi)\rho_f + \phi\rho_p,\\
(\rho C_t)_{nf} &= (1-\phi)(\rho C_t)_f + \phi(\rho C_t)_p,
\end{aligned} \tag{2.7}$$

where ϕ is the solid volume fraction. The indexes nf, f and p denote respectively nanofluid, fluid and nanosolid particles. We have

Table 1: Thermophysical properties of blood and nanoparticles.

Physical properties	Blood/base fluid	SWCNTs	Al_2O_3	TiO_2	Cu
$\rho\,(kg/m^3)$	1080	2600	3970	4250	8933
$C_p\,(J/kgK)$	3500	425	765	686.2	385
$k\,(W/mK)$	0.59	6600	40	8.953	401
$\sigma\,(s/m)$	0.6	10^6-10^7	35×10^6	2.6×10^6	59.5×10^6
$\beta\times10^{-5}\,(1/K)$	0.18	27	0.85	0.9	1.67

$$A_0 = 1-\phi+\phi\frac{\rho_p}{\rho_f}, \qquad A_5 = 1-\phi+\phi\frac{(\rho C_C)_p}{(\rho C_C)_f},$$
$$A_1 = \frac{1}{(1-\phi)^{2.5}}, \qquad A_6 = \frac{k_{nf}}{k_f},$$
$$A_2 = \frac{\sigma_p}{\sigma_f}, \qquad b_0 = \frac{b_0^*\nu_f}{A_0\rho_f U_0},$$
$$A_3 = 1-\phi+\phi\frac{(\rho\beta_T)_p}{(\rho\beta_T)_f}, \quad b_1 = \frac{b_1^*\nu_f}{A_0\rho_f U_0},$$
$$A_4 = 1-\phi+\phi\frac{(\rho\beta_C)_p}{(\rho\beta_C)_f}, \quad \omega = \frac{U_0^2}{\nu_f}\omega^*,$$

where

$$Gr = \frac{\nu_f g(\beta_T)_f(T_1^\star - T_{-\infty}^\star)}{U_0^3\rho_f} \quad \text{is the thermal Grashof number,}$$
$$G_m = \frac{\nu_f g(\beta_T)_f(C_1^\star - C_{-\infty}^\star)}{U_0^3\rho_f} \quad \text{is the mass Grashof number,}$$
$$P_r = \frac{\nu_f C_T}{k_f} \quad \text{is the Prandtl number,}$$
$$Q = \frac{Q_M\nu_f^2}{k_f U_0} \quad \text{is the heat source,}$$
$$N_t = \frac{\tau D_T(T_1^\star - T_\infty^\star)}{\nu_f T_\infty^\star} \quad \text{is the thermophoresis parameter,}$$
$$N_b = \frac{\tau D_B\,(C_1^\star - C_\infty^\star)}{\nu_f} \quad \text{is the Brownian motion,}$$
$$L_e = \frac{\nu_f}{D_b\rho_f} \quad \text{the Lewis number.}$$

In what follows, we make use of the special functions

$$L^{-1}\left\{\frac{1}{S^a+m}\right\} = F_a(-m,t) = \sum_{n=0}^{\infty}\frac{(-m)^n t^{(n+1)a-1}}{\Gamma\big(a(n+1)\big)}\,a>0, \tag{2.8}$$

$$L^{-1}\left\{\frac{S^{\gamma}}{S^{a}+m}\right\}=R_{a,\gamma}(-m,t)=\sum_{n=0}^{\infty}\frac{(-m)^{n}t^{(n+1)a-1-\gamma}}{\Gamma\big(a(n+1)-\gamma\big)}\ \mathrm{Re}(a-\gamma)>0, \tag{2.9}$$

where $F_a(.,.)$ is the Robotnov-Harley's function, and $R_{a,\gamma}(.,.)$ is the Lozenzo-Hartly's function. In the particular case $a=1$,

$$F_1(-m,t)=e^{-mt},\quad R_{1,-1}(-m,t)=\frac{1-e^{-mt}}{m}.$$

The model Eqs. (2.2)-(2.4) are associated to the initial and boundary conditions

$$\begin{array}{llll} U^*(r^*,0)=0, & U^*(0,t)=g(t), & U^*(\infty,t^*) & \rightarrow\ f(t),\\ T^*(r^*,0)=0, & T^*(0,t^*)=T_w^*, & T^*(\infty,t^*) & \rightarrow\ 0,\\ C^*(r^*,0)=0, & C^*(0,t^*)=C_w^*, & C^*(\infty,t^*) & \rightarrow\ 0, \end{array} \tag{2.10}$$

where $g(t^*)=\Psi U_0\cos(\omega^* t^*)$, Ψ is a decay parameter and

$$f(t^*)=-b_0R_{a,-1}\left(-\frac{MA_2}{A_0},t^*\right)-b_1\cos\omega t*F_a\left(-\frac{MA_2}{A_0},t^*\right).$$

The set of model Eqs. (2.2)-(2.4) can be generalized to their time-fractional versions by multiplying each of them by $\lambda=\nu_f/U_0^2$. This leads to the fractional-order equations

$$\begin{aligned}\lambda\rho_{nf}D_t^{\alpha}u^*=&-\lambda\frac{\partial p^{\star}}{\partial z}+\lambda\nu_{nf}\frac{\partial^2}{\partial r^{\star 2}}u^{\star}-\lambda\sigma_{nf}B_0^2u+\lambda g(\beta_T)_{nf}(T^{\star}-T_{\infty}^{\star})\\&+\lambda g(\beta_C)_{nf}(C^{\star}-C_{\infty}^{\star}),\end{aligned} \tag{2.11}$$

$$\lambda\left(\rho C_T\right)_{nf}D_t^{\alpha}T^*=\lambda k_{nf}\frac{\partial^2}{\partial r^{\star 2}}T^{\star}-\frac{\partial q}{\partial r^*}, \tag{2.12}$$

$$\lambda D_t^{\alpha}C^*=\lambda D_B\frac{\partial^2C^{\star}}{\partial r^{\star 2}}+\lambda\frac{D_T}{T_{\infty}^{\star}}\frac{\partial^2T^{\star}}{\partial r^{\star 2}}, \tag{2.13}$$

where

$$D_t^{\alpha}m(r,t)=\begin{cases}\dfrac{1}{\Gamma(1-a)}\displaystyle\int_0^t\frac{1}{(t-\tau)}\frac{\partial m(r,\tau)}{\partial\tau}, & 0<a<1,\\ \dfrac{\partial f(r,t)}{\partial t}, & a=1\end{cases} \tag{2.14}$$

is the fractional Caputo derivative [4,23].

Introducing the dimensionless variables

$$U^*=U_0U,\quad r^*=\frac{\nu_f}{\sqrt{\rho_f}U_0},\quad t^*=\frac{\nu_f}{U_0^2}t,\quad T=\frac{T^{\star}-T_{\infty}^{\star}}{T_1^{\star}-T_{\infty}^{\star}},\quad C=\frac{C^{\star}-C_{\infty}^{\star}}{C_1^{\star}-C_{\infty}^{\star}},$$

we get the fractionalized set of equations

$$D_t^{\alpha}U = b_0 + b_1 cos(\omega t) + \frac{A_1}{A_0}\frac{\partial^2}{\partial r^2}U - \frac{A_2}{A_0}MU + \frac{A_3}{A_0}G_r T + \frac{A_4}{A_0}G_m C, \tag{2.15}$$

$$D_t^{\alpha}T = \frac{A_7}{A_5 Pr}\frac{\partial^2}{\partial r^2}T, \tag{2.16}$$

$$D_t^{\alpha}C^* = \frac{1}{Le}\frac{\partial^2 C}{\partial r^2} + \frac{Nt}{LeN_b}\frac{\partial^2 T^{\star}}{\partial r^{\star 2}}. \tag{2.17}$$

The initial and boundary conditions (2.10) then become

$$\begin{array}{llll} U(r,0)=0, & U(0,t)=g(t), & U(\infty,t) & \rightarrow \quad f(t), \\ T(r,0)=0, & T(0,t)=1, & T(\infty,t) & \rightarrow \quad 0, \\ C(r,0)=0, & C(0,t)=1, & C(\infty,t) & \rightarrow \quad 0, \end{array} \tag{2.18}$$

where $g(t) = \Psi \cos(\omega t)$, Ψ is a decay parameter and

$$f(t) = -b_0 R_{a,-1}\left(-\frac{MA_2}{A_0}, t\right) - b_1 \cos\omega t * F_a\left(-\frac{MA_2}{A_0}, t\right).$$

3 Calculation of temperature and concentration

We apply the Laplace transform on Eq. (2.16) to obtain

$$s^a \overline{T}(r,s) = \frac{A_7}{A_5 Pr}\frac{\partial^2 \overline{T}(r,s)}{\partial r^2}, \tag{3.1}$$

where the Laplace transform is applied on the times component

$$\overline{m}(r,s) = \int_0^{\infty} m(r,t)e^{-st}\,dt. \tag{3.2}$$

Eq. (3.1) is equivalent to

$$\frac{\partial^2 \overline{T}(r,s)}{\partial r^2} - \frac{s^a A_5 Pr}{A_7}\overline{T}(r,s) = 0. \tag{3.3}$$

By writing (3.3) equivalently, under boundary conditions (2.18), we obtain

$$\overline{T}(r,s) = \frac{1}{s}\exp\left(-r\sqrt{\frac{s^a A_5 Pr}{A_7}}\right). \tag{3.4}$$

By invoking the inverse Laplace transform, we get

$$T(r,t) = \Phi\left(1, -\frac{a}{2}; -r\sqrt{\frac{s^a A_5 Pr}{A_7}}\right), \tag{3.5}$$

where

$$\Phi(\alpha,\beta;t)=\sum_{\xi=0}^{\infty}\frac{\tau^{\xi}}{\xi!\,\Gamma(\alpha+\beta\xi)}$$

is the Wright function [9].

Applying the Laplace transform to Eq. (2.17), the second derivative of $\overline{T}(r,s)$ (3.4) permits to get

$$\frac{\partial^2\overline{C}(r,s)}{\partial r^2}-Les^a\overline{C}(r,s)+\frac{1}{s}\frac{s^{a-1}N_tA_5Pr}{N_BA_7}\exp\left(-r\sqrt{\frac{s^aA_5Pr}{A_7}}\right)=0. \tag{3.6}$$

Eq. (3.5) is equivalent to

$$\begin{aligned}\overline{C}(r,s)=&\frac{1}{s}\exp\left(-r\sqrt{Le\,s^a}\right)\\&+\frac{A_5PrN_t}{N_B(LeA_7-A_5Pr)}\exp\left(-r\sqrt{\frac{s^aA_5Pr}{A_7}}\right).\end{aligned} \tag{3.7}$$

Applying the Laplace inverse transform to Eq. (3.7), we deduce

$$\begin{aligned}C(r,t)=&\Phi\left(1,-\frac{a}{2};-r\sqrt{\frac{Le}{t^a}}\right)\\&+\frac{A_5PrN_t}{N_B(LeA_7-A_5Pr)}\Phi\left(1,-\frac{a}{2};-r\sqrt{\frac{A_5Pr}{A_7t^a}}\right).\end{aligned} \tag{3.8}$$

4 Calculation of velocity

By applying the Laplace transform to Eq. (2.15), we obtain

$$\begin{aligned}&\frac{\partial^2\overline{U}(r,s)}{\partial r^2}-\left(\frac{A_0}{A_1}s^a+\frac{MA_2}{A_1}\right)\overline{U}(r,s)+\frac{b_0A_0}{sA_1}\\&+\frac{b_1A_0}{A_1}\frac{s}{s^2+\omega^2}+\frac{A_3G_r}{A_1}\overline{T}(r,s)+\frac{A_4G_m}{A_1}\overline{C}(r,s)=0\end{aligned} \tag{4.1}$$

Under boundary condition and Eqs. (3.4), (3.7), Eq. (4.1) is equivalent to

$$\begin{aligned}\overline{U}(r,s)=&\frac{\Psi s}{s^2+\omega^2}\exp\left(-r\sqrt{\frac{A_0}{A_1}s^a+\frac{MA_2}{A_1}}\right)\\&-\left(b_0+b_1\frac{s}{s^2+\omega^2}\right)\frac{1}{s^a+MA_2/A_0}\\&-A_{11}\frac{1}{s^a-MA_2/(A_1A_8)}\exp\left(-r\sqrt{s^aA_5Pr}\right)\\&-\frac{A_4Gm}{A_1A_9}\frac{1}{s^a-MA_2/(A_1A_9)}\exp\left(-r\sqrt{Le\,s^a}\right).\end{aligned}$$

Using series expansion, we write

$$\begin{aligned}
&\frac{\Psi s}{s^2+\omega^2}\exp\left(-r\sqrt{\frac{A_0}{A_1}s^a+\frac{MA_2}{A_1}}\right)\\
&=\Psi\frac{s}{s^2+\omega^2}+\Psi\frac{s}{s^2+\omega^2}\times\sum_{\zeta=1}^{\infty}\frac{\left(-r\sqrt{A_0/A_1}\right)^{\zeta}}{\zeta!}\\
&\times\sum_{\xi=0}^{\infty}\frac{(MA_2/A_0)^{\xi}\Gamma(\zeta/2+1)}{\xi!\Gamma(\zeta/2-\xi+1)}\frac{1}{s^{a\xi-a\zeta/2}}.
\end{aligned}\tag{4.2}$$

Applying inverse Laplace transform and Eq. (4.2), under boundary conditions (2.18), Eq. (4.1) is equivalent to

$$U(r,t)=U_1+U_2+U_3+U_4+U_5,\tag{4.3}$$

where

$$\begin{aligned}
U_1&=\Psi\cos(\omega t)+\Psi\cos(\omega t)\times\sum_{\zeta=1}^{\infty}\frac{(-r\sqrt{A_0/A_1})^{\zeta}}{\zeta!},\\
U_2&=t^{-(a\zeta/2+1)}\sum_{\zeta=1}^{\infty}\frac{(MA_2/A_0)^{\xi}\Gamma(\zeta/2+1)}{\xi!\Gamma(\zeta/2-\xi+1)}\Phi\left(-\frac{a}{2}\zeta,-a;t^a\right),\\
U_3&=-b_0R_{a,-1}\left(t,-\frac{MA_2}{A_0}\right)-b_1F_{a,-1}\left(t,-\frac{MA_2}{A_0}\right)\times\cos(\omega t),\\
U_4&=-\frac{A_4G_m}{A_1A_9}F_{a,-1}\left(t,\frac{MA_2}{A_1A_9}\right)\times\Phi\left(1,-\frac{a}{2};-r\sqrt{\frac{Le}{t^a}}\right),\\
U_5&=-A_{10}F_{a,-1}\left(t,\frac{MA_2}{A_1A_8}\right)\times\Phi\left(1,-\frac{a}{2};-r\sqrt{\frac{s^aA_5Pr}{A_7}}\right).
\end{aligned}$$

5 Analysis of graphical results

An analysis is presented to investigate the effects of heat and mass transfer on the transcient MHD flow on a blood. Expressions of velocity U, temperature T and concentration C are obtained by using Laplace transform method. We have made numerical simulations in order to understand the physical behavior of the magnetic parameter M, the Grashof numbers Gr and Gm, the dimensionless time t, and the Prandtl parameter Pr.

Fig. 2 presents profiles of dimensionless temperature, concentration and velocity of different nanoparticles. It is observed that single walls carbon nanotubes have a great temperature effect and concentration in blood than alumina and tin, but the inverse ef-

fect is observed for velocity.This figure shows that the exact solutions of dimensionless temperature concentration and velocity verify the initial and boundary conditions. We also notes that the present results for distribution of velocity, concentration and temperature profiles are displayed for both small and large times (see Figs. 6, 2-22).

The variation of dimensionless temperature profiles for different nanoparticles by variation of Prandtl number is presented by Fig. 4. It is observed that the transfer of mass change by the nature of nanoparticles. The increase of Prandtl number increases temperature for copper, the inverse effect is observed for tin and alumina nanoparticles.

The variation of temperature, concentration and velocity for different values of dimensionless time is shown in Fig. 3. We observe that velocity increases with the decreasing of time, which is the opposite effect for temperature and concentration of blood with single walls carbon nanotubes as base particle.

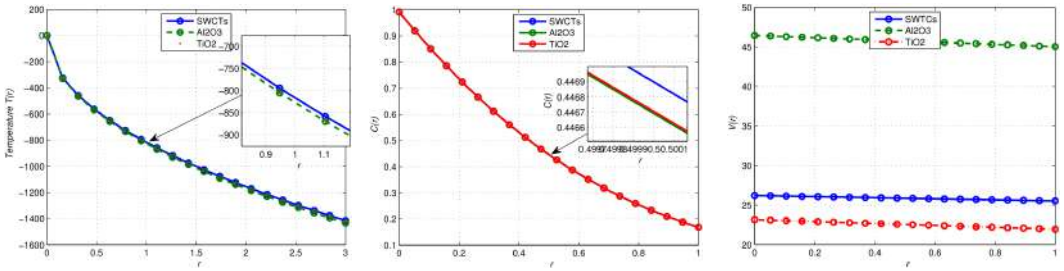

Figure 2: Profiles of temperature, concentration and velocity for different nanoparticles with $t=4$, $Pr=0.9$, $a=0.7$, $Le=0.001$, $a=0.7$, $\phi=0.05$, $\Psi=0.1$.

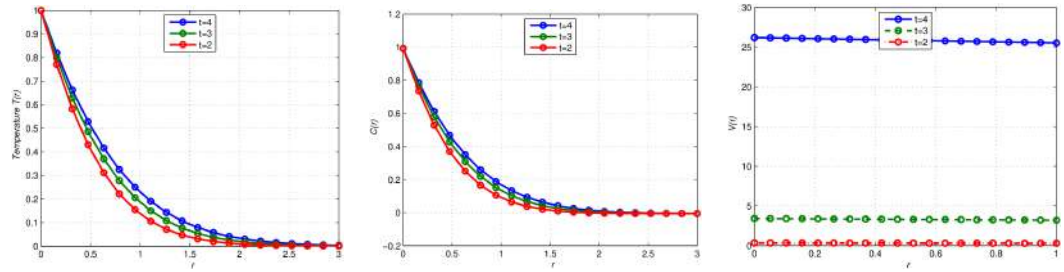

Figure 3: Profiles of temperature, concentration and velocity for SWTCs with $Pr=0.9$, $a=0.7$, $Le=0.001$, $a=0.7$, $\phi=0.05$, $\Psi=0.1$.

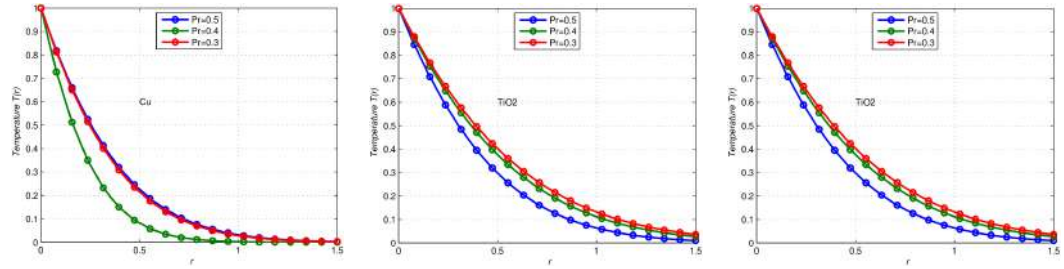

Figure 4: Profiles of temperature for different nanoparticles with a variation of Prandtl number, $t=0.6$, $a=0.7$, $\phi=0.05$, $\Psi=0.1$.

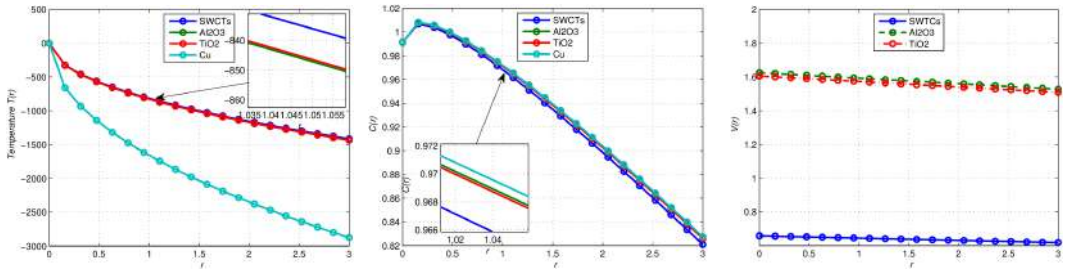

Figure 5: Profiles temperature, concentration and velocity, $a = 1$, $t = 3$, $Pr = 1$, $Le = 0.001$, $Gr = 0.001$, $Gm = 0.001$, $\phi = 0.05$, $\Psi = 0.1$.

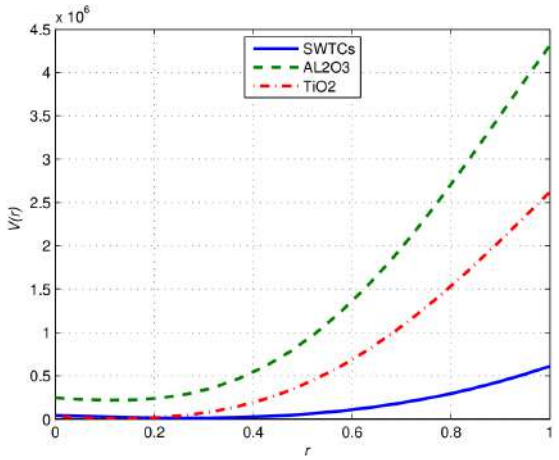

Figure 6: Profiles of velocity for a great value of time $t = 10$, $Pr = 1$, $Gr = 0.01$, $Gm = 0.001$, $Le = 0.001$, $a = 0.7$, $\phi = 0.05$, $\Psi = 0.1$.

Fig. 19 presents the velocity profile of blood with tin and copper nanoparticles for different values of the mass Grashof number. It is observed that the velocity increased with the decrease of the values of mass Grashof number. This parameter creates a Lorentz force, similar to the force created by the pressure of heart, which increase acceleration of blood flow.

Fig. 22(a) presents the velocity profile of blood with copper nanoparticles for different values of the magnetic parameter M. It is observed that velocity increases upon decreasing of magnetic parameter. This effect is the result of the Lorentz force, which accelerates the flow upon decreasing of the values of M. In the absence of magnetic field, velocity tend to be steady. Fig. 22(b) the velocity profile with copper nanoparticles for different values of the Caputo derivative parameter a. As observed by the study made by [19], the profile of velocity increased with increasing of values of a.

The effect of variation of sphericity in velocity, concentration and temperature is presented in Figs. 7-18. It is observed that according to the type of nanoparticle, behavior of velocity change under variation of sphericity of nanoparticle. But temperature decreases by the decrease of sphericity, the opposite behavior it observes in the profile of concentration.

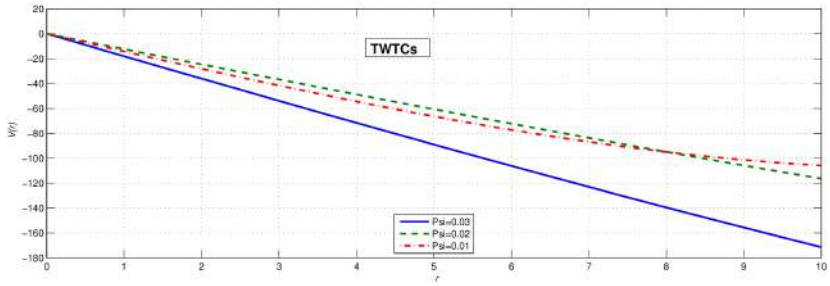

Figure 7: Profiles of velocity for SWTcS, $t = 2$, $Pr = 0.9$, $Le = 0.001$, $M = 0.01$, $b_0 = 10^{-7}$, $b_1 = 10^{-2}$, $G_m = 0, 1$, $Gr = 0, 1$, $\phi = 0.05$, $\Psi = 0.1$.

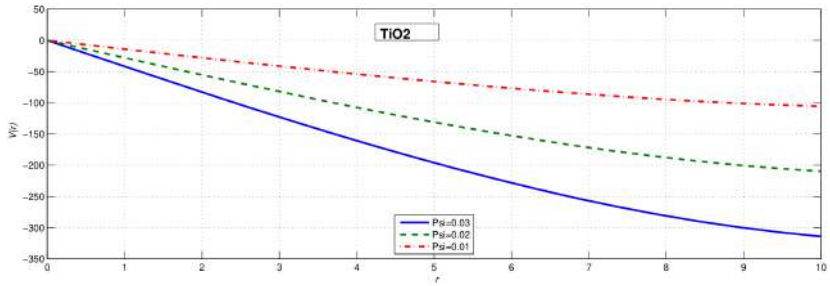

Figure 8: Profiles of velocity for TiO_2, $t = 2$, $Pr = 0.9$, $Le = 0.001$, $M = 0.01$, $b_0 = 10^{-7}$, $b_1 = 10^{-2}$, $G_m = 0, 1$, $Gr = 0, 1$, $\Psi = 0.1$.

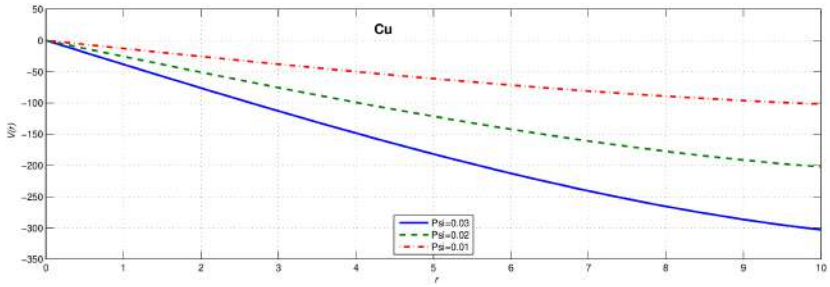

Figure 9: Profiles of velocity for Cu, $t = 2$, $Pr = 0.9$, $Le = 0.001$, $M = 0.01$, $b_0 = 10^{-7}$, $b_1 = 10^{-2}$, $G_m = 0, 1$, $Gr = 0, 1$, $\Psi = 0.1$.

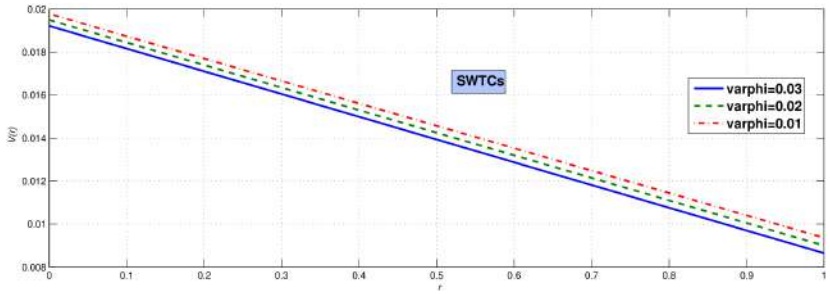

Figure 10: Profiles of velocity for SWTcS, $t = 2$, $Pr = 0.9$, $Le = 0.001$, $M = 0.01$, $b_0 = 10^{-7}$, $b_1 = 10^{-2}$, $G_m = 0, 1$, $Gr = 0.1$, $\Psi = 0.1$.

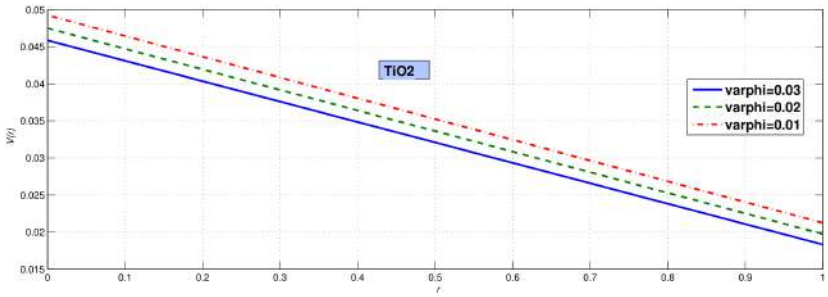

Figure 11: Profiles of velocity for TiO_2, $t=2$, $Pr=0.9$, $Le=0.001$, $M=0.01$, $b_0=10^{-7}$, $b_1=10^{-2}$, $G_m=0,1$, $Gr=0,1$, $\Psi=0.01$.

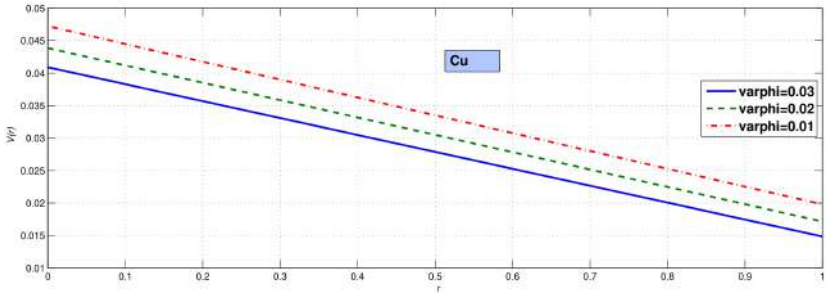

Figure 12: Profiles of velocity for Cu, $t=2$, $Pr=0.9$, $Le=0.001$, $M=0.01$, $b_0=10^{-7}$, $b_1=10^{-2}$, $G_m=0,1$, $Gr=0.1$, $\Psi=0.1$.

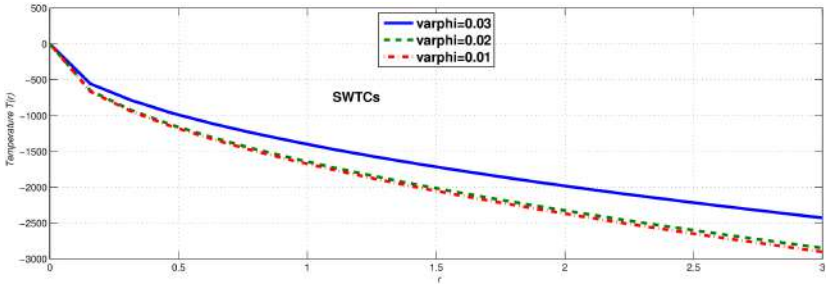

Figure 13: Profiles of temperature for SWTCs, $t=2$, $Pr=0.9$, $Le=0.001$, $M=0.01$, $b_0=10^{-7}$, $b_1=10^{-2}$, $G_m=0,1$, $Gr=0,1$, $\Psi=0.1$.

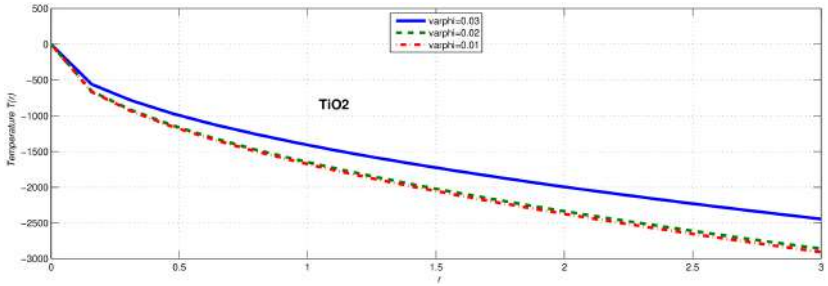

Figure 14: Profiles of temperature for TiO_2, $t=2$, $Pr=0.9$, $Le=0.001$, $M=0.01$, $b_0=10^{-7}$, $b_1=10^{-2}$, $G_m=0,1$, $Gr=0,1$, $\Psi=0.1$.

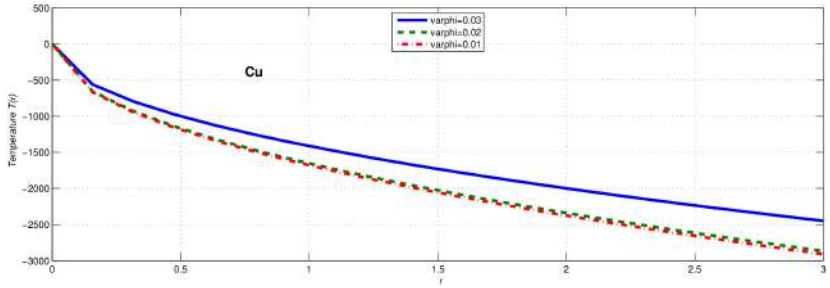

Figure 15: Profiles of temperature for Cu, $t = 2$, $Pr = 0.9$, $Le = 0.001$, $M = 0.01$, $b_0 = 10^{-7}$, $b_1 = 10^{-2}$, $G_m = 0, 1$, $Gr = 0, 1$, $\Psi = 0.1$.

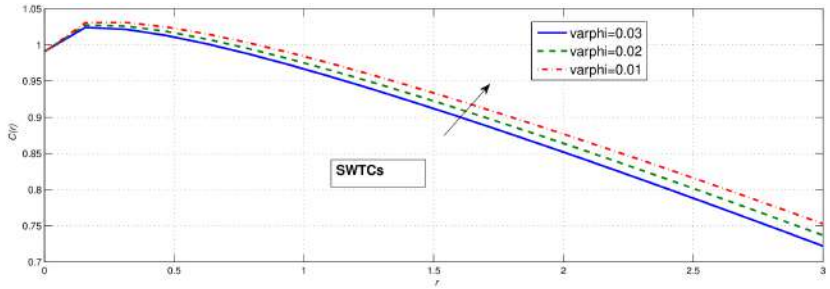

Figure 16: Profiles of concentration for SWTCs, $t = 2$, $Pr = 0.9$, $Le = 0.001$, $M = 0.01$, $b_0 = 10^{-7}$, $b_1 = 10^{-2}$, $G_m = 0, 1$, $Gr = 0, 1$, $\Psi = 0.1$.

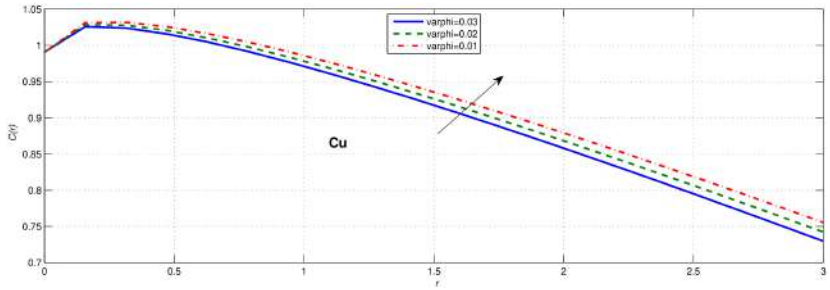

Figure 17: Profiles of concentration for Cu, $t = 2$, $Pr = 0.9$, $Le = 0.001$, $M = 0.01$, $b_0 = 10^{-7}$, $b_1 = 10^{-2}$, $G_m = 0, 1$, $Gr = 0, 1$, $\Psi = 0.1$.

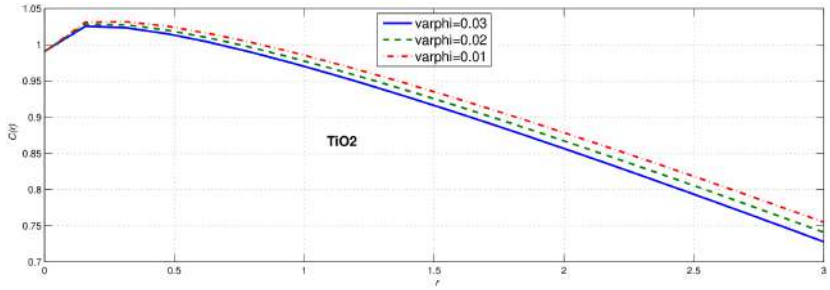

Figure 18: Profiles of concentration for TiO_2, $t = 2$, $Pr = 0.9$, $Le = 0.001$, $M = 0.01$, $b_0 = 10^{-7}$, $b_1 = 10^{-2}$, $G_m = 0, 1$, $Gr = 0, 1$, $\Psi = 0.1$.

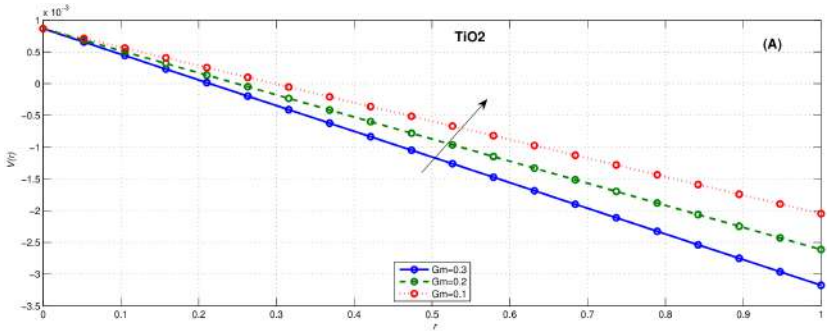

(a)

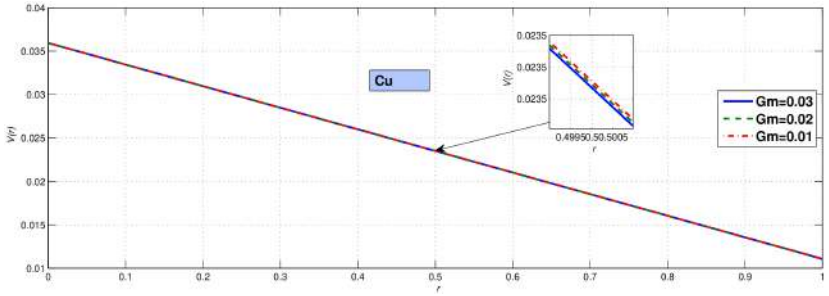

(b)

Figure 19: Profiles of velocity of Cu and TiO_2 for different mass Grashof number, $t = 4$, $Pr = 1$, $Gr = 0.01$, $Le = 0.001$, $a = 0.7$, $\phi = 0.05$, $\Psi = 0.1$.

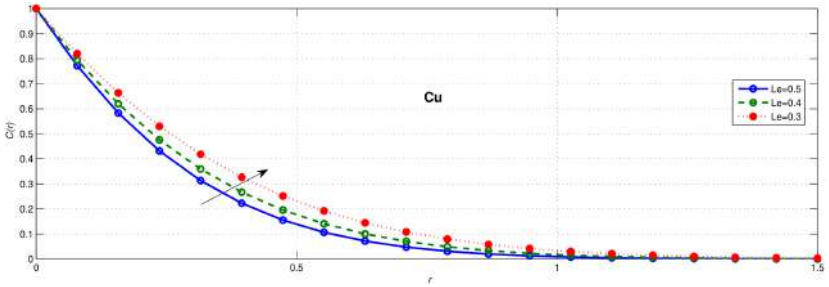

(a)

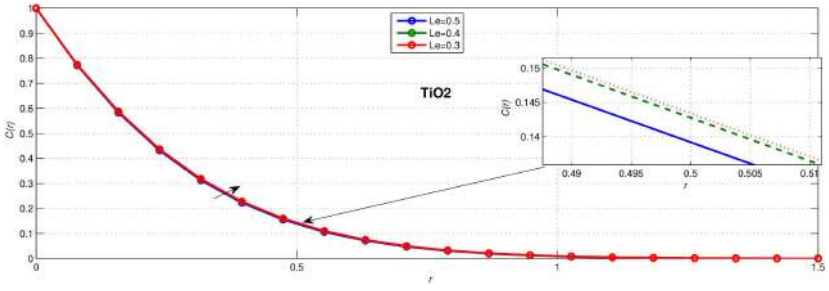

(b)

Figure 20: Profiles of concentration of Cu and TiO_2 for different values of Lewis number, $t = 4$, $Pr = 1$, $Gr = 0.01$, $Gm = 0.001$, $Le = 0.001$, $a = 0.7$, $\phi = 0.05$, $\Psi = 0.1$.

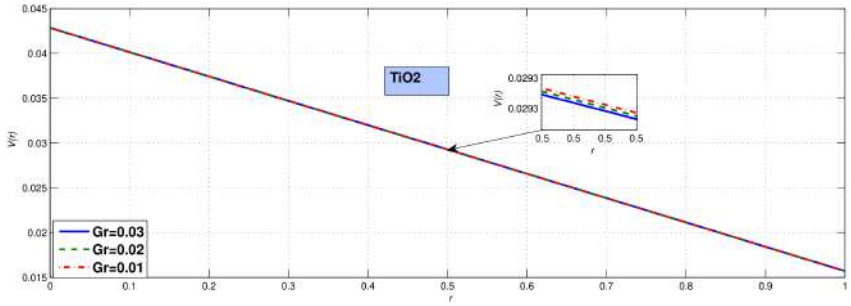

(a)

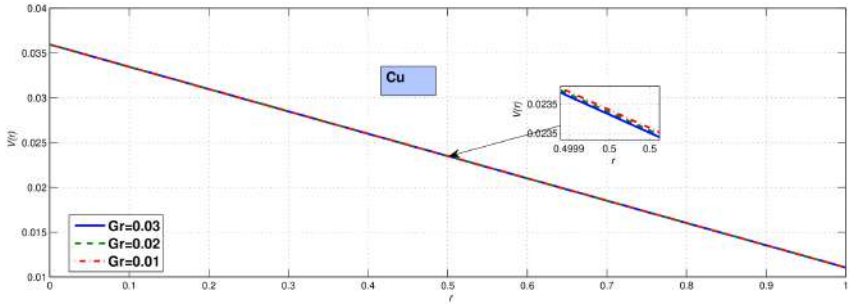

(b)

Figure 21: Profiles of velocity of Cu and TiO_2 for different thermal Grashof number, $t = 4, Pr = 1, Gm = 0.01, Le = 0.001, a = 0.7, \phi = 0.05, \Psi = 0.1$.

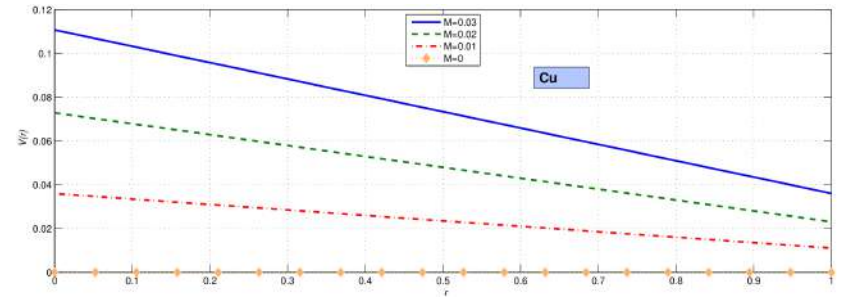

(a)

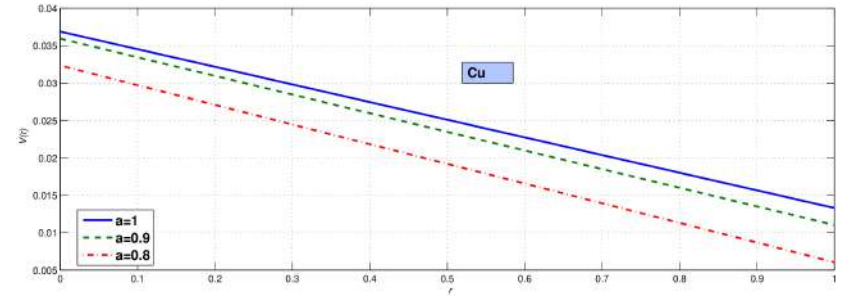

(b)

Figure 22: Profiles of velocity of Cu, $t = 3$, $Pr = 1$, $Gm = 0.01$, $Le = 0.001$, $a = 0.7$, $\phi = 0.05$, $\Psi = 0.1$.

6 Conclusion

The exact solution of a fractionalized mathematical model of unsteady concective MHD flow of blood as base fluid with single walls carbon nanotubes, Cu (convective copper), TiO_2 (tin), and Al_2O_3 (alumina) and Cu (copper) as base nanoparticles, with thermal and mass transfer, is obtained through Laplace transform with respect to time variable. The main conclusion are listed below.

(i) Single walls carbon nanotubes have a great temperature effect and concentration than alumina and tin, but the inverse effect is observed for velocity.

(ii) The increase of Prandtl number increases temperature for copper, the inverse effect is observed for tin and alumina nanoparticles.

(iii) The velocity increases with the decreasing of time, which is the opposite effect for temperature and concentration of blood with single walls carbon nanotubes as base particle.

(iv) The velocity of tin and copper as base particle increased with the decrease of the values of mass Grashof number Gm.

(v) The velocity of copper as base particle increases upon decreasing of magnetic parameter.

(vi) The behavior of velocity change under variation of sphericity of nanoparticle. But temperature decreases by the decrease of sphericity, the opposite effect it observes in the profile of concentration.

References

[1] B. Ali, Y. Nie, S. Hussain, A. Manan, and M. T. Sadiq, *Unsteady magnetohydrodynamic transport of rotating Maxwell nanofluid flow on a stretching sheet with Cattaneo-Christov double diffusion and activation energy*, Therm. Sci. Eng. Prog., 20 (2020), 100720.

[2] F. Ali, I. Khan, N. A. Sheikh, and S. Murtaza, *Heat transfer analysis of generalized Jeffery nanofluid in a rotating frame: Atangana-Balaenu and Caputo-Fabrizio fractional models*, Chaos Solit. Fractals, 129 (2019), pp. 1–15.

[3] S. Bose and M. Banerjee, *Magnetic particle capture for biomagnetic fluid flow in stenosed aortic bifurcation considering particle-fluid coupling*, J. Magn. Magn. Mater., 385 (2015), pp. 32–46.

[4] M. Caputo, *Linear model of dissipation whose Q is almost frequency independent-II*, Geophys. J. R. Astron. Soc., 13(5) (1967), pp. 529–539.

[5] L. C. Chen , W. H. Wang , W. Q. Zhu, and Z. S Li, *Stationary response of Duffing oscillator with hardening stiffness and fractional derivative*, Int. J. Non-Linear Mech., 48 (2013), pp. 44–50.

[6] S. U. Choi and J. A. Eastman, *Enhancing thermal conductivity of fluids with nanoparticle*, Technical report, Argonne National Laboratory, United States, 1995.

[7] A. C. L. Cogley , E. S. Giles, and W. G. Vincenti, *Differential approximation for radiative heat transfer in a non-grey gas near equilibrium*, American Institute of Aeronautics and Astronautics, 6(3) (1968), 551–553.

[8] K. R. CRAMER AND S. I. PAI, Magnetofluid Dynamics for Engineers and Applied Physicists, McGraw-Hill, 1973.
[9] M. EL-SHAHED AND A. SALEM, *An extension of wright function and its properties*, J. Math., 2015 (2015), 950728.
[10] R. A. FREWER, *The electrical conductivity of flowing blood*, Biomed. Eng., 9(12) (1974), pp. 552–555 .
[11] E. J. FURLANI, E. P. FURLANI, *A model for predicting magnetic targeting of multifunctional particles in the microvasculature*, J. Magn. Magn. Mater., 312 (2007), pp. 187–193.
[12] A. GAIND, I. PURI, S. SEN, AND R. GANGULY, *Analyzing ferrofluid transport for magnetic drug targeting*, J. Magn. Magn. Mater., 289 (2005), pp. 331–334 .
[13] A. HOBINY, F. ALZAHRANI, AND M. I. KHAN, *Heat transport and nonlinear mixed convective nanomaterial slip flow of Walter-B fluid containing gyrotactic microorganisms*, Alex. Eng. J., 59(3) (2020), pp. 1761–1769.
[14] A. IMTIAZ, F. ALI, I. KHAN, AND N. A. SHEIKH, *Flow of magnetic particles in blood with isothermal heating: A fractional model for two-phase flow*, J. Magn. Magn. Mater., 456 (2018), pp. 413–422.
[15] F. JASPARD AND M. NADI, *Dielectric properties of blood: An investigation of temperature dependence*, Physiol. Meas., 23(3) (2002), pp. 547–554.
[16] R. KANDASAMY, R. MOHAMAD, AND M. ISMOEN, *Impact of chemical reaction on Cu, Al_2O_3 and SWCNTs-nanofluid flow under slip conditions*, Eng. Sci. Technol. Int. J., 19 (2016), pp. 700–709.
[17] G. H. R. KEFAYATI, *Simulation of magnetic field effect on non-newtonian blood flow between two-square concentric duct annuli using FDLBM*, J. Taiwan Inst. Chem. Eng., 45(4) (2014), pp. 1184–1196.
[18] G. H. R. KEFAYATI, *FDLBM simulation of magnetic field effect on non-newtonian blood flow in a cavity driven by the motion of two facing lids*, Powder Technol., 253 (2014), pp. 325–337.
[19] A. MOHAMADOU, C. B. TABI, G. MOTSUMI, AND T. C. D. K. BANSI, *Fractional blood flow in oscillatory arteries with thermal radiation and magnetic field effects*, J. Magn. Magn. Mater., 456 (2018), pp. 38–45.
[20] A. MONDAL AND G. C. SHIT, *Transport of magneto-nanoparticles during electro-osmotic flow in a micro-tube in the presence of magnetic field for drug delivery application*, J. Magn. Magn. Mater., 442 (2017), pp. 319–328.
[21] P. MURTHY AND S. SHAW, *Magnetic drug targeting in the permeable blood vessel – The effect of blood rheology*, J. Nanotechnol. Eng. Med., 1 (2010), 021001.
[22] P. A. NDJAWA YOMI, C. D. BANSI KAMDEM, T. NKOA NKOMOM, C. B TABI, A. MOHAMADOU, AND T. C. KOFANÉ, *Fractional blood flow in rotating nanofluid with different shapes nanoparticles in the influence of activation energy and thermal radiation*, Chaos, 31 (2021), 093109.
[23] Z. ODIBAT, *Approximations of fractional integrals and Caputo fractional derivatives*, Appl. Math. Comput., 178(2) (2006), pp. 527–533.
[24] D. RAO AND K. S. R. VANI, *Effect of thermal radiation on unsteady convective heat transfer flow of a rotating nano-fluid past a vertical plate*, Adv. Appl. Sci. Res., 7 (2016), pp. 83–94 .
[25] S. SHARMA , U. SINGH, AND V. K. KATIYAR, *Magnetic field effect on flow parameters of blood along with magnetic particles in a cylindrical tube*, J. Magn. Magn. Mater., 377 (2015), pp. 395–401.
[26] E. M. SPARROW AND R. D. CESS, Radiation Heat Transfer, Hemisphere Publishing Corporation, 1978.
[27] A. SUTRADHAR, P. V. S. N. MURTHY, AND S. SHAW, *Magnetic drug targeting in an imper-*

meable microvessel with the influence of inertia of multifunctional carrier particle, J. Nanofluids, 5(5) (2016), pp. 728–735.

[28] C. B. TABI, *Fractional unstable patterns of energy in α-helix proteins with long-range interactions*, Chaos Solit. Fractals, 116 (2018), pp. 386–391.

[29] C. B. TABI, *Spatial synchrony in fractional order metapopulation cholera transmission*, Chaos Solit. Fractals, 117 (2018), pp. 37–49.

[30] E. E. TZIRTZILAKIS, *A mathematical model for blood flow in magnetic field*, Phys. Fluids, 17 (2005), 077103.

[31] H. XING , G. GAO, S. YANG, AND Y. SHEN, *Primary resonance of Duffing oscillator with fractional-order derivative*, Commun. Nonlinear Sci. Numer. Simul., 17(7) (2012), pp. 3092–3100.